Japanese Journal of Applied Physics **55**, 07MB01 (2016)
http://doi.org/10.7567/JJAP.55.07MB01

REGULAR PAPER

Effect of hotspot position fluctuation to writing capability in heated-dot magnetic recording

Warunee Tipcharoen[1], Chanon Warisarn[1]*, Arkom Kaewrawang[2], and Piya Kovintavewat[3]*

[1]*College of Data Storage Innovation, King Mongkut's Institute of Technology Ladkrabang, Bangkok 10520, Thailand*
[2]*Magnetic Materials and Data Storage Research Laboratory, Khon Kaen University, Khon Kaen 40002, Thailand*
[3]*Data Storage Technology Research Center, Nakhon Pathom Rajabhat University, Nakhon Pathom 73000, Thailand*

*E-mail: chanon.wa@kmitl.ac.th; piya@npru.ac.th

Received November 29, 2015; accepted April 15, 2016; published online June 16, 2016

This work presents the effect of hotspot position fluctuation to writing capability in heated-dot magnetic recording systems at an areal density (AD) beyond 2 Tbpsi via a micromagnetic modeling. At high ADs, the hotspot and the write field gradient may not be correctly focused on the target island because the bit islands are closely positioned to one another. This may lead to the overwriting/erasing of the previously written islands, which can severely affect the recording performance. Therefore, this work studies the 3-by-3 data patterns that easily cause an error when the hotspot and write head positions are fluctuated by various island pitches. Simulation results indicate that the data pattern that leads to the highest/lowest error occurrence frequency is the one with the first, second and fourth islands having the opposite/same magnetization direction to/as the write field, regardless of the magnetization direction of the third island. This result can, for example, be utilized to design a two-dimensional modulation code to prevent such destructive data patterns, thus helping enhance the overall system performance.

1. Introduction

The next generation of magnetic recording technology has been expected to capable of storing digital data at multi-terabit per square inch (Tbpsi).[1,2] Heated-dot magnetic recording (HDMR) is one of the promising technologies to achieve an ultra-high recording density,[3] because it can prevent the transition noise caused by zig-zag grain boundary, and can improve the writability by temporarily reducing the coercivity of magnetic media.[4–6]

HDMR is a new technology that combines many techniques employed in heat assisted magnetic recording (HAMR),[7] bit-patterned media recording (BPMR),[8] shingled magnetic recording (SMR),[9] and two-dimensional magnetic recording (TDMR).[10] However, there are still many parameters that limit an achievable storage capacity,[5,11] such as hotspot position fluctuation, the recorded-bit data patterns,[12–15] and so on. Recently, BPMR with a lollipop near field transducer is investigated at about 1 Tbpsi. In practice, the optical spot on the patterned media is better concentrated than that on the continuous media. Additionally, the produced hotspot size has been lower below 100 nm and it can be reduced by adjusting curved edges at the bottom of the peg.[3]

Practically, the inappropriate thermal distribution and write head field gradient that cover the neighboring recorded bits in both the along- and across-track directions can cause a written-in error during the writing process.[3,11,16] Therefore, the effect of hotspot position fluctuation needs to be investigated, and the durability of recorded-bit patterns against this effect must be understood before writing the data onto a magnetic medium. In this work, the position jitters of hotspot and write head field have been examined by the realistic micromagnetic modeling based on a finite difference (FD) method.[17]

2. Micromagnetic modeling and writing process

This paper considers an island size of $10 \times 10 \times 10\,\mathrm{nm}^3$ and an island pitch of 17, 15, and 13 nm, which correspond to the areal densities (ADs) of 2.2, 2.8, and 3.8 Tbpsi, respectively. Because the bit islands become smaller, the thermal stability must be compensated by utilizing a high anisotropy material such as $L1_0$-FePt.[18] Nevertheless, this work considers the material $L1_0$-FePt with a magnetocrystalline anisotropy constant (K_u) of $4.6\,\mathrm{MJ/m}^3$ and a saturation magnetization constant (M_s) of 1125 kA/m,[19] which can be obtained by a magnetron sputtering method. Note that these values allow the minimum stable grain size of about 2.8 nm at a thermal stability of 60.[19] In addition, an intradot exchange coupling is set to be 12 pJ/m.[20,21]

The micromagnetic modeling procedure and how to evaluate thermal effect on bit-patterned media via the Landau–Lifshitz–Gilbert (LLG) equation[21,22] can be summarized as follows.

a) To generate a bit-patterned medium, we consider the island size and pitch as mentioned above, which are used to specify the geometric volumes of spaces or regions. Each island region has a different easy axis that declines in range of 0–20° with Gaussian distribution.

b) To create the magnetization state for all possible data patterns as listed in the Table I, which is used to define the initial magnetization of a medium before the fifth island is being written. Note that this paper assumes that the first–fourth islands are the previously recorded bits (i.e., there are 16 possible data patterns), and the fifth–ninth islands are initially assumed to be the bit "−1".

c) To produce the write head field contour, the triangular write pole is utilized with trailing and side shields, whose dimension is 93.5 nm wide (along-track) and 50.5 nm long (across-track) as shown in Fig. 1. The write field gradient in the along-track direction is 500 Oe/nm, whereas that in the across-track direction is 483 Oe/nm.[23,24] After the magnetic field amplitude was carefully investigated, we found that its maximum value should be greater than or at least equal to 20 kOe so as to obtain the error percentage (will be defined in Sect. 3) below 10%.

d) To gradually reduce media coercivity, the heat from a laser should be applied, where a thermal profile is Gaussian in both directions according to[25]

Table I. Illustration of all possible patterns of four previously recorded bits.

Track	Pattern 1			Pattern 2			Pattern 3			Pattern 4		
Previous track	−1	−1	−1	1	−1	−1	−1	−1	1	1	−1	1
Current track	−1	−1	−1	−1	−1	−1	−1	−1	−1	−1	−1	−1
Next track	−1	−1	−1	−1	−1	−1	−1	−1	−1	−1	−1	−1

Track	Pattern 5			Pattern 6			Pattern 7			Pattern 8		
Previous track	1	−1	1	−1	1	−1	1	1	−1	−1	1	1
Current track	1	−1	−1	−1	−1	−1	−1	−1	−1	−1	−1	−1
Next track	−1	−1	−1	−1	−1	−1	−1	−1	−1	−1	−1	−1

Track	Pattern 9			Pattern 10			Pattern 11			Pattern 12		
Previous track	1	1	1	−1	−1	−1	1	−1	−1	−1	−1	1
Current track	−1	−1	−1	1	−1	−1	1	−1	−1	1	−1	−1
Next track	−1	−1	−1	−1	−1	−1	−1	−1	−1	−1	−1	−1

Track	Pattern 13			Pattern 14			Pattern 15			Pattern 16		
Previous track	−1	1	−1	1	1	−1	−1	1	1	1	1	1
Current track	1	−1	−1	1	−1	−1	1	−1	−1	1	−1	−1
Next track	−1	−1	−1	−1	−1	−1	−1	−1	−1	−1	−1	−1

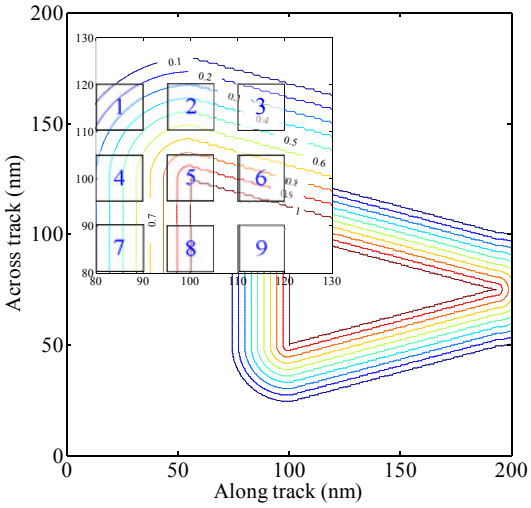

Fig. 1. (Color online) Write head field contour modeled with the maximum amplitude of 20 kOe,[23] where the corner is used to magnetize the fifth island.

$$T = T_0 \exp\left(-\frac{r^2}{r_0^2}\ln 2\right), \tag{1}$$

where T is the temperature (K), T_0 is the maximum temperature (K), r is the distance (m), and r_0 is the full width at half maximum of the thermal profile (m). Finally, a thermal spot size of 70 nm is considered in this work, as demonstrated in Fig. 2 (not scaled).[26]

Because the $L1_0$-FePt material is employed as a recording layer of a bit-patterned medium and its Curie temperature, T_C, is 750 K,[20,27] then the highest recording temperature should

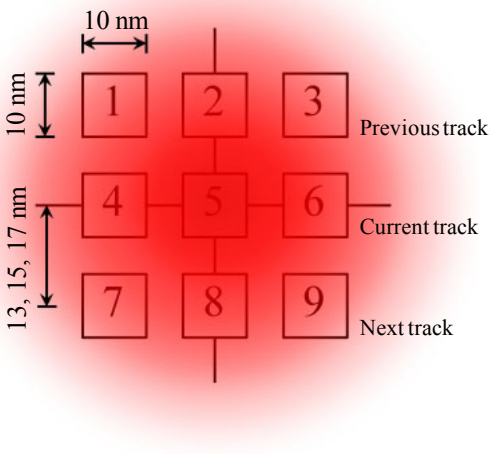

Fig. 2. (Color online) The island layout with $10 \times 10 \times 10\,\text{nm}^3$ bit volume heated by the Gaussian thermal profile (FWHM = 70 nm).

be lower than this limit. In addition, Chen et al.[28] have tested and measured an erasure temperature of $L1_0$-FePt HAMR media for a laser heating method. They found that the old data can be completely erased at the temperature of 650 K with the laser power of 72 mW. Thus, 650 K is set to be the maximum temperature (at a nucleus) for the writing process, where a room temperature is 293 K.

Because we cannot compute the thermal effect directly from the LLG equation, the Brillouin function is then taken into account for M_s calculation under the thermal effect according to (in CGS unit)[29,30]

$$M_s(T) = M_s(0)\left[\frac{2J+1}{2J}\coth\left(\frac{2J+1}{2J}\beta\right) - \frac{1}{2J}\coth\left(\frac{\beta}{2J}\right)\right], \tag{2}$$

where $M_s(0)$ is the M_s at room temperature, J is a total angular momentum assumed to be 0.85, and β is defined as

$$\beta = 3\left(1 - \frac{T}{T_C}\right), \tag{3}$$

and T_C is set to be 750 K.

After $M_s(T)$ is achieved, $K_u(T)$ can then be obtained from

$$\frac{K_u(T)}{K_u(0)} = \left[\frac{M_s(T)}{M_s(0)}\right]^n, \tag{4}$$

where $K_u(0)$ is the K_u at room temperature, and n is about 2 according to the parameters of $Fe_{55}Pt_{45}$.[19]

Figure 3 demonstrates the dependence of M_s and K_u on the temperature T, where both M_s and K_u decrease as T increases. This means that the magnetic property of a magnetic material declines and it appears to be paramagnetic at T_C. In addition, the summation of magnetic moment vectors is approximately zero when the magnetic field disappears. As a result, we have modeled the writing process by using the thermal profile and the bit-patterned medium, where the K_u and M_s of magnetic islands are calculated with different values corresponding to the thermal profile expansion.

Furthermore, the heat and magnetic field pulses are assumed to be constant every moment, where they are applied until the energy of a torque term in the LLG equation is lower than 0.01 A/m.[31] Consequently, the calculation should be

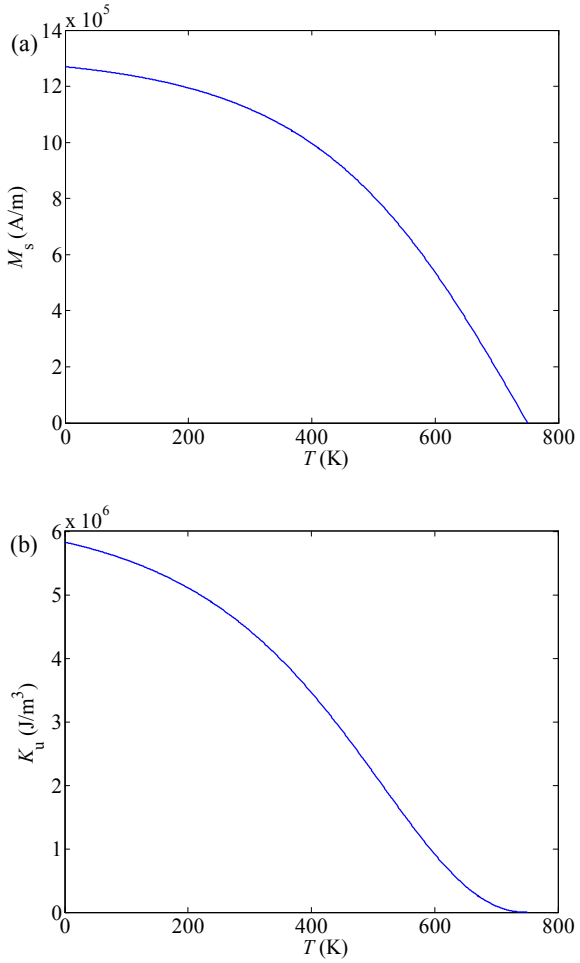

Fig. 3. (Color online) Dependence of (a) M_s and (b) K_u on the temperature T plotted via the Brillouin function.[29)]

considered complete. It should be pointed out that the torque criterion is employed for determining a writing duration, and a switching time will not be considered in this work.

To study the effect of hotspot and head field contour position fluctuations, their deviations are modeled as a Gaussian random variable. Additionally, the thermal profile covers all 9 islands in both along- and across-track directions as illustrated in Fig. 2. Then, the magnetic field of the triangular head corner is applied to write the data on the center bit (i.e., the fifth island) to be the bit "+1", as demonstrated in Fig. 1. It is very important to note that the micromagnetic modeling is performed using the OOMMF package[31)] based on the LLG equation, which has been solved by the FD method, where the FD mesh used in the calculation is $0.5 \times 0.5 \times 10\,\mathrm{nm}^3$.

3. Results and discussion

To identify results after the writing process, the principles of a magnetization reversal after the writing process should be described first. The magnitude of magnetic moment vectors across all spins in an individual island and magnetic domain are considered to be a criterion for a magnetization reversal. Such a measured magnitude from an individual bit should be above 50% of M_s, where it is decided to be a complete magnetization switching. The magnetic domain is also realized, which must be consistent with another one to be double checked. Other cases will be decided to be an

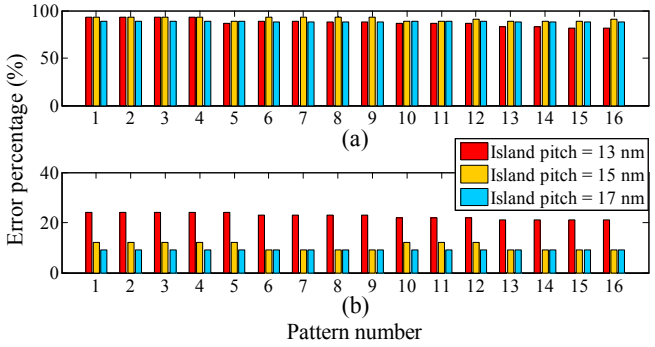

Fig. 4. (Color online) Error percentage as a function of data patterns at three different ADs; (a) the hotspot and the main pole are moved together within all nine islands' area, and (b) both of the hotspot and the write head positions are moved over the target island's area (the fifth island).

incomplete magnetization reversal. We use this result to specify two different states, i.e., bit "+1" and "−1".

The writing performance can be evaluated based on the above definition. Moreover, an error is defined as the error occurred from the writing process under heat, which can be classified into two conditions. Firstly, the error occurs when some previously recorded data are magnetized into different states by the write head that is currently writing a bit on the target island (i.e., the fifth island). Secondly, the error happens when the bit cannot be recorded onto the target island because of a drastic inaccuracy of hotspot and write pole positions. For example, for each data pattern (see Table I), we rewrite the bit on the target island for 100 rounds. After recording the target bit, we evaluate the error according to the criteria mentioned above. Then, for each round, if any or both of the two conditions have occurred, it will be counted as one error. Therefore, for each data pattern, the sum of all errors will be multiplied by 100% to obtain "an error percentage".

3.1 Worst case of position fluctuations

The center of the hotspot position is fluctuated with respect to a main pole, which can move to any location within nine islands. For each data pattern based on the previously recorded bits, we apply the magnetic field to write the bit "+1" on the fifth island, and then investigate the written-in error that might have occurred within the surrounding bits (caused by the thermal expansion).

Figure 4(a) shows the error percentage as a function of data patterns at three different ADs. Clearly, they have an error percentage close to one another and the maximum one is close to 90%. The main cause of this error comes from the target island that could not be recorded. Furthermore, it seems that the thermal and head field gradients may lead to overwriting in some previously written tracks and bits (mostly in the second and fourth islands) because of severe position fluctuation and large thermal spot size.

Additionally, we found that when the magnetization directions of the second and fourth islands are opposite to the direction of the write field, it will definitely cause the written-in error. The error percentage can be decreased when the second or fourth island has the same magnetization direction with the write field (i.e., same as the magnetization direction of the fifth island). Moreover, when the second and

fourth islands have the same magnetization direction with the write field, it will yield the lowest error percentage.

3.2 Position deviation improvement

To approach the "error free" in the HDMR writing process and to make the simulation model more realistic, the fluctuations of hotspot and head positions are adjusted to be within the target island's area. Figure 4(b) demonstrates that the error percentage greatly drops and decreases below 10% for the island pitches of 15 and 17 nm, while the error percentage drops to around 21–24% for the island pitch of 13 nm. Although the position fluctuation has been improved, the cause of error is still similar to that described in Sect. 3.1. To obtain a lower error percentage, the deviation of hotspot and head positions should be smaller than the island area. In this case, the second and fourth islands are often overwritten, which is resulted from a very high write field gradient even if an island pitch is increased. In addition, we also found that the cause of error from the first and third islands may be neglected because the thermal distribution and the write field gradient that cover these bits are insufficient.

Decreasing the hotspot size is also one of the choices to prevent the written-in error, which depends on the optical design. Because the shingled writing technology is used, the hotspot and head position can move in any direction while the target island is being written. Thus, optimizing the thermal profile and the write field gradient should also be taken into consideration.

Consequently, given the optimal writing temperature and write head field gradient, the written-in error in HDMR systems can be alleviated by avoiding some data patterns to be written onto a medium. This can be achieved by applying a two-dimensional modulation code on the input data before recording as proposed in Ref. 32.

4. Conclusions

The written-in error occurred during the writing process of HDMR has been studied using a realistic micromagnetic simulation at the AD beyond 2 Tbpsi. Simulation results show that the error percentage is increased with a decrease of island pitch (i.e., AD is increased). Then, to reduce this error, the position deviation has been improved by allowing the hotspot position to move within the target island's area. The other ways to decrease the error during the writing process include using a smaller hotspot size, writing the media at lower temperature, and utilizing the two-dimensional modulation code to prevent the data pattern that easily cause a written-in error.

Acknowledgments

This work was supported in part by College of Data Storage Innovation KMITL, Thailand Research Fund (TRF), and in part by Research and Development Institute, Nakhon Pathom Rajabhat University, Thailand.

1) F. Wang and X.-H. Xu, Chin. Phys. B **23**, 036802 (2014).
2) D. Weller, G. Parker, O. Mosendz, E. Champion, B. Stipe, X. Wang, T. Klemmer, G. Ju, and A. Ajan, IEEE Trans. Magn. **50**, 3100108 (2014).
3) A. Ghoreyshi and R. H. Victora, J. Appl. Phys. **115**, 17B719 (2014).
4) R. F. L. Evans, R. W. Chantrell, U. Nowak, A. Lyberatos, and H. J. Richter, Appl. Phys. Lett. **100**, 102402 (2012).
5) R. Wood, J. Magn. Magn. Mater. **321**, 555 (2009).
6) Y. Shiroishi, K. Fukuda, I. Tagawa, H. Iwasaki, S. Takenoiri, and H. Tanaka, IEEE Trans. Magn. **45**, 3816 (2009).
7) R. E. Rottmayer, S. Batra, D. Buechel, W. A. Challener, J. Hohlfeld, Y. Kubota, L. Li, B. Lu, C. Mihalcea, K. Mountfield, K. Pelhos, C. Peng, T. Rausch, M. A. Seigler, D. Weller, and X. M. Yang, IEEE Trans. Magn. **42**, 2417 (2006).
8) H. J. Richter, A. Y. Dobin, R. T. Lynch, D. Weller, R. M. Brockie, O. Heinonen, K. Z. Gao, J. Xue, R. J. M. v. d. Veerdonk, P. Asselin, and M. F. Erden, Appl. Phys. Lett. **88**, 222512 (2006).
9) F. Lim, B. Wilson, and R. Wood, IEEE Trans. Magn. **46**, 1548 (2010).
10) K. S. Chan, J. J. Miles, E. Hwang, B. V. K. Vijayakumar, J.-G. Zhu, W.-C. Lin, and R. Negi, IEEE Trans. Magn. **45**, 3837 (2009).
11) M. H. Kryder, E. C. Gage, T. W. McDaniel, W. A. Challener, R. E. Rottmayer, J. Ganping, Y. T. Hsia, and M. F. Erden, Proc. IEEE **96**, 1810 (2008).
12) Y. Wang, R. H. Victora, and B. V. K. Vijaya Kumar, IEEE Trans. Magn. **51**, 3001505 (2015).
13) R. Wood, Y. Sonobe, Z. Jin, and B. Wilson, J. Magn. Magn. Mater. **235**, 1 (2001).
14) D. Niarchos, Sens. Actuators A **109**, 166 (2003).
15) S. N. Piramanayagam, J. Appl. Phys. **102**, 011301 (2007).
16) H. Ye, V. Sng, C. Du, J. Zhang, and G. Guo, IEEE Trans. Magn. **38**, 2180 (2002).
17) J. E. Miltat and M. J. Donahue, in *Handbook of Magnetism and Advanced Magnetic Materials*, ed. H. Kronmuller and S. Parkin (Wiley, New York, 2007) p. 742.
18) J.-U. Thiele, S. Maat, and E. E. Fullerton, Appl. Phys. Lett. **82**, 2859 (2003).
19) J.-U. Thiele, K. R. Coffey, M. F. Toney, J. A. Hedstrom, and A. J. Kellock, J. Appl. Phys. **91**, 6595 (2002).
20) J. Zhang, Y. Liu, F. Wang, J. Zhang, R. Zhang, Z. Wang, and X. Xu, J. Appl. Phys. **111**, 073910 (2012).
21) W. Tipcharoen, A. Kaewrawang, and A. Siritaratiwat, Adv. Mater. Sci. Eng. **2015**, 504628 (2015).
22) T. Schrelf, J. Fidler, D. Suess, W. Scholz, and V. Tsiantos, in *Handbook of Advanced Magnetic Materials: Micromagnetic Simulation of Dynamic and Thermal Effects*, ed. Y. Liu, D. J. Sellmyer, and D. Shindo (Springer, Heidelberg, 2006) p. 129.
23) M. Yamashita, Y. Okamoto, Y. Nakamura, H. Osawa, K. Miura, S. J. Greaves, H. Aoi, Y. Kanai, and H. Muraoka, IEEE Trans. Magn. **48**, 4586 (2012).
24) M. Yamashita, Y. Okamoto, Y. Nakamura, H. Osawa, K. Miura, S. Greaves, H. Aoi, Y. Kanai, and H. Muraoka, J. Appl. Phys. **111**, 07B727 (2012).
25) B. X. Xu, Z. J. Liu, R. Ji, Y. T. Toh, J. F. Hu, J. M. Li, J. Zhang, K. D. Ye, and C. W. Chia, J. Appl. Phys. **111**, 07B701 (2012).
26) B. X. Xu, Z. Cen, J. H. Goh, J. Li, K. Ye, J. Zhang, H. Yang, Y. T. Toh, and C. Quan, IEEE Trans. Magn. **49**, 2559 (2013).
27) S. Okamoto, N. Kikuchi, O. Kitakami, T. Miyazaki, Y. Shimada, and K. Fukamichi, Phys. Rev. B **66**, 024413 (2002).
28) Y. J. Chen, H. Z. Yang, S. H. Leong, K. M. Cher, J. F. Hu, P. Sethi, and W. S. Lew, J. Appl. Phys. **117**, 17D117 (2015).
29) F. Akagi, M. Mukoh, M. Mochizuki, J. Ushiyama, T. Matsumoto, and H. Miyamoto, J. Magn. Magn. Mater. **324**, 309 (2012).
30) F. Akagi, T. Matsumoto, and K. Nakamura, J. Appl. Phys. **101**, 09H501 (2007).
31) M. J. Donahue and D. G. Porter, OOMMF User's Guide, Version 1.0, Interagency Report NISTIR 6376 (National Institute of Standards and Technology, Gaithersburg, MD, 1999).
32) A. Arrayangkool and C. Warisarn, J. Appl. Phys. **117**, 17A904 (2015).

